Methylxanthine derivative-rich cacao extract suppresses differentiation of adipocytes through downregulation of PPARγ and C/EBPs

Yoko YAMASHITA[1,†], Takakazu MITANI[1,2,†], Liuqing WANG[1] and Hitoshi ASHIDA[1*]

[1] *Department of Agrobioscience, Graduate School of Agricultural Science, Kobe University, 1-1 Rokkodai-cho, Nada-ku, Kobe 6578501, Japan.*
[2] *Department of Interdisciplinary Genome Sciences and Cell Metabolism, Institute for Biomedical Sciences, Interdisciplinary Cluster for Cutting Edge Research, Shinshu University, 8304 Minamiminowa, Kamiina, Nagano 399-4598, Japan.*

Running head: Cacao extract suppresses adipocyte differentiation
The number of characters: 30,948
The number of figures: 7
The number of tables: 2

† YY and TM contributed equally to the study.

[*]**To whom all correspondence should be addressed:** Dr. Hitoshi Ashida, Department of Agrobioscience, Graduate School of Agricultural Science, Kobe University, 1-1 Rokkodai-cho, Nada-ku, Kobe 6578501, Japan. TEL & FAX: 81-78-803-5878
e-mail: ashida@kobe-u.ac.jp

Abbreviations: ACC, acetyl CoA carboxylase; AMPK, AMP-activated protein kinase; C/EBPs, CCAAT/enhancer-binding proteins; DMEM, Dulbecco's modified Eagle's medium; DMI, dexamethasone, 3-isobutyl-1-methylxanthine, insulin; FAS, fatty acid synthase; PBS, phosphate-buffered saline; PPARγ, peroxisome proliferator-activated receptor gamma; qPCR, quantitative PCR; SREBP1, sterol regulatory element-binding protein 1.

Summary

Cacao extract (CE) consumption has beneficial effects on human health, such as lowering the risk of obesity. However, the underlying molecular mechanism for the anti-obesity effect of CE remains incompletely understood. Here, we used a 50% aqueous alcohol extract of cacao mass, which is rich in methylxanthine derivatives (about 11%) and poor in flavan-3-ols (less than 1%), and assessed the suppression effects of this extract on adipocyte differentiation to investigate the anti-obesity mechanism. CE dose-dependently decreased fat accumulation in 3T3-L1 cells without affecting cell viability. CE also dose-dependently decreased the protein and gene expression levels of two adipogenesis-related transcription factors, peroxisome proliferator-activated receptor gamma (PPARγ) and CCAAT/enhancer-binding proteins (C/EBPs). Moreover, CE decreased protein expression levels of sterol regulatory element-binding protein 1 (SREBP1) and its downstream fatty acid synthase (FAS), which was accompanied by the retained localization of SREBP1 in the cytoplasm of 3T3-L1 cells. After ICR mice were fed a diet containing 1% CE for 1 week, their white adipose tissue weight was lower, whereas their brown adipose tissue weight was higher compared with those of control animals. Additionally, the protein expression levels of PPARγ, C/EBPs, SREBP-1, and FAS in the white adipose tissue of these mice were also lower than those in control animals. In contrast, diet

supplementation with CE induced higher levels of phosphorylated AMP-activated protein kinase (AMPK) and its downstream acetyl-CoA carboxylase. In conclusion, methylxanthine derivative-rich CE decreases fat accumulation in adipocytes by downregulating the expression of the adipocyte differentiation master regulators through the activation of AMPK.

Key Words: cacao; methylxanthine derivatives; PPARγ; C/EBPs; adipocyte differentiation

Introduction

Obesity is linked to the increased onset of certain chronic diseases, such as diabetes and cardiovascular diseases (*1-4*). Under the condition of obesity, adipocytes accumulate abnormal or excessive fat. Since adipocyte differentiation is acutely involved in fat accumulation (*5*), controlling adipocyte differentiation is a promising strategy for the prevention of obesity.

During differentiation from fibroblast-like preadipocytes to mature adipocytes, peroxisome proliferator-activated receptor gamma (PPARγ) and CCAAT/enhancer-binding proteins (C/EBPs) are the master regulators or crucial determinants of adipocyte fate (6). AMP-activated protein kinase (AMPK) is a key modulator for maintaining both the cellular and whole-body energy balance (*7*). The activation of AMPK inhibits the differentiation of 3T3-L1 cells by downregulating the expression of PPARγ and C/EBPs (*8*). Moreover, activated AMPK interacts with sterol regulatory element binding protein 1 (SREBP1) and inhibits the expression of its target molecule, fatty acid synthase (FAS), leading to a reduction of lipogenesis and lipid accumulation (*9-11*), in addition to promoting phosphorylation of acetyl CoA carboxylase (ACC) and inhibiting its activity (*12*).

Certain food materials and phytochemicals have been reported to reduce the risk of obesity (*13-16*). Intake of cacao liquor

or dark chocolate ameliorates and/or prevents obesity in humans (*17-18*). Cacao-derived flavan-3-ol-rich extract has also been shown to prevent obesity in animal studies (*19*). Cacao liquor and its flavan-3-ols decrease the plasma cholesterol level (*20*). In addition to flavan-3-ols, cacao also contains methylxanthine-derivatives such as theobromine and caffeine, and these compounds likewise perform functions that are beneficial to human health (*21*). A recent study reported that caffeine and catechins improve lipid metabolism synergistically through an AMPK-dependent action in mice fed a high-fat diet (*22*). These results indicate that cacao extract (CE) and its components possess anti-obesity effects. However, the underlying molecular mechanism for the anti-obesity effect of CE, particularly the effect of a methylxanthine derivative-rich CE, is not yet fully understood.

In this study, we investigated that expression of PPARγ and C/EBPs and of their downstream adiposity-related factors, SREBP1 and FAS, in 3T3-L1 adipocytes after treatment with a methylxanthine-rich CE. To confirm the observed anti-obesity effect of this extract, we fed mice a diet supplemented with CE for 7 d, and their expression levels of PPARγ, C/EBPs, SREBP1, and FAS were assessed. Moreover, we also examined the phosphorylation of AMPK as an upstream factor involved in the expression of PPARγ and C/EBPs.

Materials and Methods

Materials Methylxanthine derivative-rich CE was kindly gifted from Glico Co, Ltd, Osaka, Japan. Briefly, cacao mass produced in the Republic of Ghana (3.6 kg) was defatted with hexane, and the residue (1.6 kg) was extracted with 50% (v/v) aqueous ethanol at 80 ºC for 4 h. The obtained extract was concentrated *in vacuo* and freeze-dried. The CE yield was 286 g (7.9% cacao mass), and the CE contained 10.0% theobromine, 0.71% caffeine, 0.41% (−)-epicatechin, 0.24% (+)-catechin, 0.19% procyanidin B2, 0.13% procyanidin C1, and trace amounts of cinnamtannin A2 and other unidentified compounds.

Dulbecco's modified Eagle's medium (DMEM) was purchased from Nissui Pharmaceutical (Tokyo, Japan). Calf serum and fetal bovine serum (FBS) were obtained from Gibco BRL (Gaithersburg, MD) and Biological Industries (Kibbutz Beit Haemek, Israel), respectively. Antibodies against β-actin, PPARγ, C/EBPα, C/EBPβ, C/EBPδ, and SREBRP1, horseradish peroxidase-conjugated anti-rabbit IgG, and anti-goat IgG were purchased from Santa Cruz Biotechnology (Santa Cruz, CA), and antibodies against p-AMPK, AMPK, p-ACC, and ACC were purchased from Cell Signaling Technology (Beverly, MA). Anti-rabbit Alexa 488-conjugated antibody was purchased from Molecular Probes (Eugene, OR).

151 *Cell culture* 3T3-L1 preadipocytes were maintained in DMEM
152 supplemented with 10% calf serum, 100 µg/mL streptomycin, and
153 100 units/ml of penicillin. Adipocyte differentiation was induced as
154 described previously (*23*). Briefly, 1 d after reaching confluence,
155 the cells were treated with a DMI (10 µg/mL insulin, 1 µmol/L
156 dexamethasone, and 0.5 mmol/L 3-isobutyl-1-methylxanthine)
157 cocktail in DMEM-high glucose (4.5 g/L glucose) supplemented with
158 10% FBS and the above antibiotics for 2 d. During differentiation,
159 the cells were treated with 10 µg/mL insulin every 2 d.
160
161 *Sudan II staining* Intracellular lipid accumulation was stained
162 with Sudan II. Adipocyte differentiation was induced in 3T3-L1
163 cells via treatment with a DMI cocktail for 6 d. Determination of
164 lipid accumulation in 3T3-L1 cells was performed by Sudan II
165 staining as described previously (*24*).
166
167 *Cell viability assay* Cell viability was determined by crystal
168 violet staining assays, as described previously (*24*). Briefly, 3T3-L1
169 cells were incubated with the indicated concentrations of CE in the
170 presence of DMI for 72 h. The cells were fixed with 4%
171 paraformaldehyde in phosphate-buffered saline (PBS) for 20 min at
172 room temperature and stained with 0.2% (w/v) crystal violet in 2%
173 v/v ethanol for 10 min at room temperature. The cells were washed,
174 and the dye was extracted with 0.5% (w/v) SDS in 50% (v/v)

175 ethanol. The absorbance was measured at 570 nm with a reference
176 wavelength at 630 nm.
177
178 *Immunofluorescence microscopy* 3T3-L1 cells were differentiated
179 via treatment with DMI in the presence or absence of CE at 100
180 μg/mL for 6 d. The cells were fixed with 4% paraformaldehyde in
181 PBS for 20 min and permeabilized with 0.1% (w/v) Triton X-100 in
182 PBS for 5 min at room temperature. The cells were incubated with
183 rabbit polyclonal anti-SREBP1 antibody at 4 °C overnight, followed
184 by incubation with Alexa 488-conjugated anti-rabbit antibody. The
185 nuclei were counterstained with 4′,6-diamidino-2-phenylindole
186 dihydrochloride (DAPI) at 1 μg/mL. Fluorescent images were
187 acquired with an Olympus FSX100 fluorescence microscope
188 (Olympus, Tokyo, Japan).
189
190 *Quantitative PCR (qPCR)* Total RNA was extracted from 3T3-L1
191 cells using TRIzol (Invitrogen), and cDNA was synthesized using
192 reverse transcriptase. The resulting cDNA was subjected to qPCR
193 using the following primers: *Gapdh* (forward primer 5′-
194 ACAACTTTGGCATTGTGGAA-3′ and reverse primer 5′-
195 GATGCAGGGATGATGTTCTG-3′); *Pparg* (forward primer 5′-
196 ACGTGCAGCTACTGCATGTGA-3′ and reverse primer 5′-
197 AGAAGGAACACGTTGTCAGCG-3′); and *Cebpa* (forward primer 5′-
198 GGAACTTGAAGCACAATCGATC-3′ and reverse primer 5′-

199 TGGTTTAGCATAGACGTGCACA-3′). qPCR was performed via a
200 two-step PCR method on a Thermal Cycler Dice real-time system
201 (Takara Bio. Inc., Shiga, Japan). Ct values were transformed into
202 relative quantification data by the $2^{-\Delta\Delta Ct}$ method, and data were
203 normalized to *Gapdh* as an endogenous control.
204
205 *Western blot analysis* Cell lysate preparation and Western
206 blotting were performed as described in our previous reports (*16,*
207 *24*). Specific immune complexes were detected with the ATTO
208 Light-Capture II Western Blotting Detection System. The density of
209 specific bands was calculated using ImageJ image analysis software
210 (National Institutes of Health, Bethesda, MD).
211
212 *Animal treatment* All animal experiments were approved by the
213 Institutional Animal Care and Use Committee (Permission #27-05-
214 09) and were performed according to the Guidelines for Animal
215 Experiments set by Kobe University. Male ICR mice (4 weeks old, n
216 = 10) were obtained from Japan SLC (Shizuoka, Japan) and kept in a
217 temperature-controlled room (23 ± 2 °C) with a 12:12-h light/dark
218 cycle (lights were turned on at 9:00 am). The mice had free access
219 to tap water and an AIN-93 M laboratory-purified diet (Oriental
220 Yeast, Tokyo, Japan) and were acclimatized for 7 d before use in
221 experiments. The provided food was changed every other day. The
222 mice were then randomly divided into two groups of five and fed a

223 diet containing 0% or 1% CE and the tap water for another 7 d.

224 At the end of the experiment, the mice were sacrificed at 9:00
225 after a 15-h fast. Exsanguination via cardiac puncture was
226 performed under anesthesia using sevoflurane as an inhalational
227 anesthetic and sodium pentobarbital as an analgesic. Blood was
228 collected in a heparinized tube. Plasma was then prepared by
229 centrifugation at 800 × *g* for 10 min at 4 °C and subjected to
230 measurements of glucose, total cholesterol, and triacylglycerol
231 levels using corresponding commercial kits (Lab assay™ Glucose
232 Wako kit, Cholesterol-E test, and Triglyceride-E test, respectively,
233 all from Wako Pure Chemical Industries, Ltd.). The plasma
234 adiponectin level was measured using a commercial enzyme-linked
235 immunosorbent assay (ELISA) kit (Mouse/Rat High Molecular
236 Weight Adiponectin ELISA Kit from Shibayagi, Gunma, Japan). The
237 liver, white adipose tissue (mesenteric, epididymal, perirenal, and
238 subcutaneous adipose tissues), and brown adipose tissue were
239 collected, washed with 1.15% (w/v) KCl, weighed, immediately
240 frozen using liquid nitrogen, and kept at −80 °C until use.
241 Mesenteric white adipose tissue was used for the measurement of
242 protein expression of adipogenesis- and lipid metabolism-related
243 factors by Western blot analysis.

244

245 *Statistical analysis* All data are presented as the means ± SE (n =
246 3 for in vitro cell culture experiments and n = 5 for in vivo animal

experiments). Statistical significance was analyzed by one-way ANOVAs with a Turkey's post-hoc test for in vitro cell culture experiments or by Student's *t*-tests for in vivo animal experiments. Statistical analyses were performed with JMP statistical software version 11.2.0 (SAS Institute. Cary, NC). Differences with a $p < 0.05$ were considered statistically significant.

Results

To examine the effect of CE on adipogenesis in 3T3-L1 cells, the cells were differentiated via treatment with DMI in the presence of CE for 6 days. Intracellular lipid accumulation was visualized by staining with Sudan II (Fig. 1A, top panels). DMI treatment induced a significantly higher lipid content in 3T3-L1 cells compared with undifferentiated controls [DMI(-)], and the DMI-induced lipid accumulation was suppressed by CE in a concentration-dependent manner (Fig. 1A, bottom panel). To evaluate whether the lower lipid accumulation was due to a reduction in cell viability, a crystal violet staining assay was performed. The results show that CE had no influence on the cell viability of 3T3-L1 cells at the indicated concentrations (Fig. 1B). These results suggest that CE suppresses lipid accumulation during adipocyte differentiation without affecting cell viability.

Fig. 1

To clarify the underlying mechanism responsible for the CE-

271 induced suppression of lipid accumulation in adipocytes, we
272 investigated whether CE suppressed the expression of PPARγ and
273 C/EBPα, which are the master regulators of adipogenesis (*5*, *6*). As
274 expected, DMI treatment induced higher expression levels of PPARγ
275 and C/EBPα (Fig. 2A). Concentrations of CE above 50 μg/ml
276 suppressed the DMI-induced increase in the expression levels of
277 these proteins. CE also suppressed the DMI-induced increase in the
278 mRNA expression levels of these proteins in a concentration-
279 dependent manner (Fig. 2B). We further investigated the effect of
280 CE on the expression levels of C/EBPβ and C/EBPδ proteins, which
281 are upstream transcriptional factors of PPARγ and C/EBPα (5, *6*).
282 When 3T3-L1 cells were differentiated with DMI for 24 h,
283 significantly higher protein expression levels of C/EBPβ and
284 C/EBPδ were observed compared with those of control cells (Fig. 3).
285 CE decreased the DMI-induced expression of these proteins in a
286 concentration-dependent manner, and a statistically significant
287 decrease was observed at 50 and 100 μg/mL of CE for C/EBPβ and
288 C/EBPδ, respectively. These results indicate that the reduced
289 expression of PPARγ and C/EBPs is involved in the CE-induced
290 suppression of lipid accumulation in adipocytes.
291 We next examined expression of the downstream factors of
292 PPARγ and C/EBPs. SREBP1 is a transcription factor that regulates
293 the expression of lipogenic genes, such as FAS and low-density
294 lipoprotein receptor (*11*). As shown in Fig. 4A, DMI treatment

Fig. 4

Fig. 4

295 induced markedly higher protein expression levels of SREBP1 and
296 FAS compared with those of controls. CE-treatment significantly
297 prevented the DMI-induced expression of these proteins at
298 concentrations above 50 μg/mL (Fig. 4A). SREBP1 is activated
299 through the protease-processing pathway, and activated SREBP1
300 enters the nucleus and induces the expression of its target genes,
301 including FAS (*11*). We further analyzed the localization of SREBP1
302 in 3T3-L1 cells by immunofluorescence microscopy. In the absence
303 of CE, SREBP1 is localized in both the cytoplasm and nucleus (Fig.
304 4B, top panels). However, in the presence of 100 μg/mL CE,
305 SREBP1 was mainly localized in the cytoplasm (Fig. 4B, bottom
306 panels). From these results, we confirm that the CE-induced
307 reduction in PPARγ and C/EBPs expression levels results in the
308 suppression of SREBP1 and FAS expression.
309 Lastly, we performed in vivo experiments to confirm the
310 results obtained from the in vitro cell-culture experiments. Diet
311 supplementation with 1% CE for 7 d resulted in less body weight
312 gain and lower total white adipose tissue weights in male ICR mice
313 compared with control mice (Table 1), without altering the amount
314 of food intake (control: 3.68 ± 0.34 g/day/head vs. CE: 3.33 ±
315 0.37 g/day/head). In contrast, brown adipose tissue weight was
316 slightly, but significantly, higher in the mice that had consumed CE.
317 Although the plasma glucose and total cholesterol levels remained
318 similar between the two groups, the plasma triacylglycerol level

Table 1

following CE supplementation was only about 50% of that in the control animals (Table 2). Interestingly, after CE supplementation, the mice also had a higher level (1.45-fold) of plasma adiponectin compared with control animals. Table 2

Although the mesenteric white adipose tissue weight was not significantly lower in animals following CE supplementation, this tissue produces the highest levels of monocyte chemoattractant protein-1 in obese mice (*25*), which indicates that, among all types of white adipose tissue, mesenteric white adipose tissue plays the most important role in obesity. Thus, mesenteric white adipose tissue was used in the ensuing experiments. The protein expression of PPARγ and C/EBPs was measured in mesenteric white adipose tissue. As shown in Fig. 5, supplementation with 1% CE for 7 d resulted in significantly lower levels of PPARγ, C/EBPα, and C/EBPβ protein expression compared with controls. However, the level of C/EBPδ expression following CE supplementation remained similar to that in control mice. Supplementation with CE also produced lower levels of protein expression of SREBP1 and FAS, which are the downstream factors for PPARγ and C/EBPs (Fig. 6). AMPK is known to inhibit adipocyte differentiation as an upstream factor of PPARγ and C/EBPs (*8*). CE supplementation induced significantly higher levels of AMPK phosphorylation and of the downstream ACC in mesenteric white adipose tissue compared with controls (Fig. 7). From these in vivo results, we conclude that CE Fig. 7 Fig. 5 Fig. 6

intake suppresses the expression of adipocyte differentiation markers via AMPK activation.

Discussion

Since obesity is involved in the increased onset of many diseases, much attention has been focused on targeting food components that may help prevent obesity. For obesity prevention by food components, the following strategies appear promising: inhibition of adipocyte differentiation (*5*), modulation of lipid metabolism (inhibition of lipogenesis and promotion of lipolysis) (*26*), and promotion of energy expenditure, including the formation of beige adipocytes (*27*). Various food materials and food-derived phytochemicals have been reported to inhibit adipocyte differentiation (*23*, *24*, *28*, *29*). In this study, we found that CE containing abundant methylxanthine derivatives decreased both lipid accumulation in 3T3-L1 cells (Fig. 1) and adipose tissue weight in mice (Table 1). Reduced expression levels of PPARγ and C/EBPs were found to be involved in the anti-adipogenic mechanism of CE (Figs. 2, 3, and 5). Additionally, because phosphorylation of AMPK has been reported to inhibit expression of PPARγ and C/EBPs (*8*), we examined AMPK phosphorylation in vivo (Fig.7), and we found that this is also involved in the anti-adipogenic mechanism of CE. Thus, CE possesses anti-adipogenic effect via reducing the

expressions of PPARγ and C/EBPs. The results of our in vivo experiments are consistent with those from our in vitro experiments, indicating that the CE mechanism observed in vitro likely contributes to the prevention of obesity in vivo.

PPARγ and C/EBPs play pivotal roles in adipocyte differentiation and adipogenesis (*7*, *30*, *31*). PPARγ forms a heterodimer with retinoic acid X-receptor (RXR) (*32*) and regulates the transcription of adipocyte-specific genes (*33*). C/EBPα functions as another principal player in adipogenesis and is most abundant in mature adipocytes (*34*). C/EBPβ and C/EBPδ are known to induce the expression of PPARγ and C/EBPα (*35, 36*). In this study, CE did not suppress protein expression of C/EBPδ in the mesenteric white adipose tissue of mice (Fig. 5), even though it significantly suppressed C/EBPδ in 3T3-L1 adipocytes (Fig. 3). Our previous report demonstrated that Ashitaba calcones, 4-hydroxyderricin and xanthoangelol, downregulate the expression of C/EBPα and PPARγ accompanied by a decrease in the expression of C/EBPβ but not in that of C/EBPδ (*23*). These results suggest that C/EBPδ is not critical for the induction of PPARγ and C/EBPα expression.

As an upstream factor for C/EBPβ, the activation of AMPK is likely also involved in the mechanism for CE induced effects. It was previously reported that AMPK activation inhibited the differentiation of 3T3-L1 cells by downregulating the expression of C/EBPs and PPARγ (*8*). Our earlier report also demonstrated that an

391 AMPK inhibitor compound C prevented the Ashitaba calcones-
392 induced downregulation of C/EBPβ, C/EBPα, and PPARγ (*23*).
393 Moreover, activated AMPK interacts with SREBP1 and inhibits the
394 expression of its target molecule FAS, leading to a reduction of
395 lipogenesis and to lipid accumulation (*9-11*). The activation of
396 AMPK may contribute to the increased level of adiponectin in
397 plasma, given that an AMPK activator is able to promote
398 adiponectin multimerization in 3T3-L1 adipocytes (*37*). However,
399 the target molecule of CE is still unclear, and further study is
400 needed to clarify this issue.
401 The anti-obesity effects of CE are well-documented. For
402 example, the intake of cacao liquor such as dark chocolate decreases
403 BMI in humans (*17, 18*), and cacao liquor procyanidins ameliorate
404 lipid metabolism in mice (*19*). Many researchers have focused on
405 cacao polyphenols, particularly flavan-3-ols, as the active
406 compounds. However, the polyphenol content in the CE used here
407 was less than 1%, whereas this extract contained abundant
408 methylxanthines, such as 10.0% theobromine and 0.71% caffeine.
409 Based on the above composition, 28 μmol/L theobromine and 1.8
410 μmol/L caffeine exist in the minimum concentration of CE (50
411 μg/mL) that is effective for the inhibition of lipid accumulation.
412 Recently, Jang et al. (*38*) reported that theobromine reduced
413 adipogenesis in 3T3-L1 cells through the suppression of AMPK and
414 ERK signaling at a concentration of 150 μg/mL (=877 μmol/L). A

human study demonstrated that plasma concentrations of theobromine increase to 28.75 μmol/L after consumption of 850 mg of theobromine for 4 weeks (*39*). Another report showed that the maximum plasma concentration of theobromine in humans is approximately 50 μmol/L (*40*). Our recent data show that theobromine above concentrations of 25 μmol/L exhibits an anti-adipogenic effect accompanied by lower expression of PPARγ and C/EBPs in 3T3-L1 adipocytes (*41*). Thus, theobromine is a strong candidate for the effective compound in CE.

Caffeine suppresses the intracellular lipid accumulation of 3T3-L1 adipocytes after full differentiation (*42*). Furthermore, coffee containing caffeine inhibits adipocyte differentiation through the inactivation of PPARγ (*43*). Recently, Kim et al. (*44*) demonstrated that caffeine at 1 mmol/L inhibits the expression of C/EBPβ, C/EBPα, and PPARγ during 3T3-L1 preadipocyte differentiation through the AKT/glycogen synthase kinase 3β pathway. In contrast, our results demonstrate that caffeine indirectly suppresses lipid accumulation in 3T3-L1 adipocytes by decreasing secretion of inflammatory cytokines from Caco-2 cells, even though direct treatment of 3T3-L1 cells with 50 mmol/L caffeine did not affect lipid accumulation (*41*). These results indicate that caffeine at a physiological concentration does not affect adipocyte differentiation, but it is possible for this compound to inhibit adipocyte differentiation at higher, non-physiological

concentrations. In the present study, CE inhibited adipocyte differentiation not only in 3T3-L1 adipocytes but also in the adipose tissue of mice. Furthermore, the caffeine concentration in CE is too low to possess an anti-adipogenic effect in 3T3-L1 cells. Thus, caffeine must not be the effective compound in CE.

In conclusion, methylxanthine-rich CE inhibits adipocyte differentiation through an AMPK-induced reduction in the expression of PPARγ and C/EBPs. Thus, methylxanthine-rich CE is an attractive novel food material with which to suppress obesity. To clarify the detailed mechanism of this effect, experiments are in progress using a methylxanthine compound.

Acknowledgments

We thank Katie Oakley, PhD, from Edanz Group (www.edanzediting.com/ac) for editing a draft of this manuscript.

References

1) Kaul K, Tarr JM, Ahmad SI, Kohner EM, Chibber R. 2012. Introduction to diabetes mellitus. *Adv Exp Med Biol* **771:** 1-11.
2) Vernooij, JW, van der Graaf Y, Visseren FL, Spiering W; On behalf of the SMART study group. 2012. The prevalence of obesity-related hypertension and risk for new vascular events in patients with vascular diseases, *Obesity* **20:** 2118-2123.

463 *3*) Vucenik I, Stains JP. 2012. Obesity and cancer risk: evidence,
464 mechanisms, and recommendations *Ann N Y Acad Sci* **1271:** 37-
465 43.
466 *4*) Ligibel J. 2011. Obesity and breast cancer. *Oncology* **25:** 994-
467 1000.
468 *5*) Cristancho AG, Lazar MA. 2011. Forming functional fat: a
469 growing understanding of adipocyte differentiation, *Nat Re.*
470 *Mol Cell Biol* **12**: 722-734.
471 *6*) Gregoire FM, Smas CM, Sul HS. 1998. Understanding adipocyte
472 differentiation. *Physiol Rev* **78**: 783-809.
473 *7*) Hardie DG, Ross FA, Hawley SA. 2012. AMPK: a nutrient and
474 energy sensor that maintains energy homeostasis. *Nat Rev Mol*
475 *Cell Biol* **13:** 251-262.
476 *8*) Gao Y, Zhou Y, Xu A, Wu D. 2008. Effects of an AMP-activated
477 protein kinase inhibitor, compound C, on adipogenic
478 differentiation of 3T3-L1 cells. *Biol Pharm Bull* **31:** 1716-1722.
479 *9*) Brown MS, Goldstein JL. 1997. The SREBP pathway: regulation
480 of cholesterol metabolism by proteolysis of a membrane-bound
481 transcription factor. *Cell* **89:** 331-340.
482 *10*) Li Y, Xu S, Mihaylova MM, Zheng B, Hou X, Jiang B, Park O,
483 Luo Z, Lefai E, Shyy JY, Gao B, Wierzbicki M, Verbeuren TJ,
484 Shaw RJ, Cohen RA, Zang M.2011. AMPK phosphorylates and
485 inhibits SREBP activity to attenuate hepatic steatosis and
486 atherosclerosis in diet-induced insulin-resistant mice. *Cell*

Metab **13:** 376-388.

11) Gosmain Y, Dif N, Berbe V, Loizon E, Rieusset J, Vidal H, Lefai E. 2005. Regulation of SREBP-1 expression and transcriptional action on HKII and FAS genes during fasting and refeeding in rat tissues. *J Lipid Res* **46:** 697-705.

12) Zhou G, Myers R, Li Y, Chen Y, Shen X, Fenyk-Melody J, Wu M, Ventre J, Doebber T, Fujii N, Musi N, Hirshman MF, Goodyear LJ, Moller DE. 2001. Role of AMP-activated protein kinase in mechanism of metformin action. *J Clin Invest* **108:** 1167-1174.

13) Rayalam S, Della-Fera MA, Baile CA.2008. Phytochemicals and regulation of the adipocyte life cycle. *J Nutr Biochem* **19:** 717-726.

14) Alappat L, Awad AB. 2010. Curcumin and obesity: evidence and mechanisms. *Nutr Rev* **68:** 729-738.

15) Ueda M, Ashida H. 2012. Green tea prevents obesity by increasing expression of insulin-like growth factor binding protein-1 in adipose tissue of high-fat diet-fad mice. *J Agric Food Chem* **60:** 8917-8923.

16) Yamashita Y, Wang L, Wang L. Tanaka Y. Zhang T. Oolong, black and pu-erh tea suppresses adiposity in mice via activation of AMP-activated protein kinase. *Food Funct* **5:** 2420-2429.

17) Golomb BA, Koperski S, White HL.2012. Association Between More Frequent Chocolate Consumption and Lower Body Mass

511 Index. *Arch Intern Med* **172:** 519-521.
512 *18*) Cuenca-García M, Ruiz JR, Ortega FB, Castillo MJ; HELENA
513 study group. 2014. Association between chocolate consumption
514 and fatness in European adolescents. *Nutrition* **30:** 236-239.
515 *19*) Yamashita Y, Okabe M, Natsume M, Ashida H. 2012. Prevention
516 mechanisms of glucose intolerance and obesity by cacao liquor
517 procyanidin extract in high-fat diet-fed C57BL/6 mice. *Arch*
518 *Biochem Biophys* **527:** 95-104.
519 *20*) Yasuda A, Natsume M, Sasaki K, Baba S, Nakamura Y, Kanegae
520 M, Nagaoka S. 2008. Cacao procyanidins reduce plasma
521 cholesterol and increase fecal steroid excretion in rats fed a
522 high-cholesterol diet. *Biofactors* **33:** 211-223.
523 *21*) Kim J, Kim J, Shim J, Lee CY, Lee KW, Lee HJ. 2014. Cocoa
524 Phytochemicals: Recent Advances in Molecular Mechanisms on
525 Health. *Crit Rev Food Sci Nutr* **54:** 1458-1472.
526 *22*) Zhao Y, Yang L, Huang Z, Lin L, Zheng G. 2017. Synergistic
527 effects of caffeine and catechins on lipid metabolism in
528 chronically fed mice via the AMP-activated protein kinase
529 signaling pathway. *Eur J Nutr* DOI 10.1007/s00394-016-1271-4.
530 *23*) Zhang T, Sawada K, Yamamoto N, Ashida H. 2013. 4-
531 Hydroxyderricin and xanthoangelol from Ashitaba (*Angelica*
532 *keiskei*) suppress differentiation of preadiopocytes to
533 adipocytes via AMPK and MAPK pathways. *Mol Nutr Food Res*
534 **57:** 1729-1740.

24) Furuyashiki T, Nagayasu H, Aoki Y, Bessho H, Hashimoto T, Kanazawa K, Ashida H. 2004. Tea catechin suppresses adipocyte differentiation accompanied by down-regulation of PPARgamma2 and C/EBPalpha in 3T3-L1 cells. *Biosci Biotechnol Biochem* **68:** 2353-2359.

25) Yu R, Kim CS, Kwon BS, Kawada T. 2006. Mesenteric adipose tissue-derived monocyte chemoattractant protein-1 plays a crucial role in adipose tissue macrophage migration and activation in obese mice. *Obesity (Silver Spring)* **14:** 1353-1362.

26) Rupasinghe HP, Sekhon-Loodu S, Mantso T, Panayiotidis MI. 2016. Phytochemicals in regulating fatty acid β-oxidation: Potential underlying mechanisms and their involvement in obesity and weight loss. *Pharmacol Ther* **165:** 153-163.

27) Vargas-Castillo A, Fuentes-Romero R, Rodriguez-Lopez LA, Torres N, Tovar AR. 2017. Understanding the Biology of Thermogenic Fat: Is Browning A New Approach to the Treatment of Obesity? *Arch Med Res* doi: 10.1016/j.arcmed.2017.10.002

28) Takahashi T, Tabuchi T, Tamaki Y, Kosaka K, Takikawa Y, Satoh T. 2009. Carnosic acid and carnosol inhibit adipocyte differentiation in mouse 3T3-L1 cells through induction of phase2 enzymes and activation of glutathione metabolism. *Biochem Biophys Res Commun* **382:** 549-554.

559 *29*) Lai CS, Tsai ML, Badmaev V, Jimenez M, Ho CT, Pan MH. 2012.
560 Xanthigen suppresses preadipocyte differentiation and
561 adipogenesis through down-regulation of PPARγ and C/EBPs
562 and modulation of SIRT-1, AMPK, and FoxO pathways. *J Agric*
563 *Food Chem* **60:**1094-1101.
564 *30*) Lefterova MI, Zhang Y, Steger DJ, Schupp M, Schug J,
565 Cristancho A, Feng D, Zhuo D, Stoeckert CJ, Liu XS, Lazar
566 MA. 2008. PPARgamma and C/EBP factors orchestrate
567 adipocyte biology via adjacent binding on a genome-wide scale.
568 *Genes Dev* **22:** 2941-2952.
569 *31*) Lefterova MI, Lazar MA. 2009. New developments in adipoge-
570 nesis. *Trends Endocrinol Metab* **20:** 107–114.
571 *32*) Kliewer SA, Umesono K, Noonan DJ, Heyman RA, Evans RM.
572 1992. Convergence of 9-cis retinoic acid and peroxisome
573 proliferator signalling pathways through heterodimer formation
574 of their receptors. *Nature* **358:** 771-774.
575 *33*) Tontonoz P, Graves RA, Budavari AI, Erdjument-Bromage H, Lui
576 M, Hu E, Tempst P, Spiegelman BM. 1994. Adipocyte-specific
577 transcription factor ARF6 is a heterodimeric complex of two
578 nuclear hormone receptors, PPAR gamma and RXR alpha.
579 *Nucleic Acids Res* **22:** 5628-5634.
580 *34*) Wu Z, Rosen ED, Brun R, Hauser S, Adelmant G, Troy AE,
581 McKeon C, Darlington GJ, Spiegelman BM. 1999. Cross-
582 regulation of C/EBPα and PPARγ controls the transcriptional

583 pathway of adipogenesis and insulin sensitivity. *Mol Cell* **3:**
584 151-158.
585 *35*) Wu Z, Bucher NL, Farmer SR. 1996. Induction of peroxisome
586 proliferator-activated receptor γ during the conversion of 3T3
587 fibroblasts into adipocytes is mediated by C/EBPβ, C/EBPδ, and
588 glucocorticoids. *Mol Cell Biol* **16:** 4128-436.
589 *36*) Rosen ED, Walkey CJ, Puigserver P, Spiegelman BM. 2000.
590 Transcriptional regulation of adipogenesis. *Genes Dev* **14:**
591 1293-1307.
592 *37*) Wang Y, Zhang Y, Wang Y, Peng H, Rui J, Zhang Z, Wang S, Li
593 Z. 2017. WSF-P-1, a novel AMPK activator, promotes
594 adiponectin multimerization in 3T3-L1 adipocytes. *Biosci*
595 *Biotechnol Biochem*. **81**:1529-1535.
596 *38*) Jang YJ, Koo HJ, Sohn EH, Kang SC, Rhee DK, Pyo S. 2015.
597 Theobromine inhibits differentiation of 3T3-L1 cells during the
598 early stage of adipogenesis via AMPK and MAPK signaling
599 pathways. *Food Funct* **6:** 2365-2374.
600 *39*) Neufingerl N, Zebregs YE, Schuring EA, Trautwein EA. 2013.
601 Effect of cocoa and theobromine consumption on serum HDL-
602 cholesterol concentrations: a randomized controlled trial. *Am J*
603 *Clin Nutr* **97:** 1201-1209.
604 *40*) Ptolemy AS, Tzioumis E, Thomke A, Rifai S, Kellogg M. 2010.
605 Quantification of theobromine and caffeine in saliva, plasma
606 and urine via liquid chromatography-tandem mass spectrometry:

a single analytical protocol applicable to cocoa intervention studies. *J Chromatogr B Analyt Technol Biomed Life Sci* **878:** 409-416.

41) Mitani T, Watanabe S, Yoshioka Y, Katayama S, Nakamura S, Ashida H. 2017. Theobromine suppresses adipogenesis through enhancement of CCAAT-enhancer-binding protein β degradation by adenosine receptor A1. Biochim Biophys Acta **1864**: 2438-2448.

42) Nakabayashi H, Hashimoto T, Ashida H, Nishiumi S, Kanazawa K. 2008. Inhibitory effects of caffeine and its metabolites on intracellular lipid accumulation in murine 3T3-L1 adipocytes. *Biofactors* **34:** 293–302.

43) Aoyagi R, Funakoshi-Tago M, Fujiwara Y, Tamura H. 2014. Coffee Inhibits Adipocyte Differentiation via Inactivation of PPARγ. *Biological and Pharmaceutical Bulletin* **37:** 1820-1825.

44) Kim HJ, Yoon BK, Park H, Seok JW, Choi H, Yu JH, Choi Y, Song SJ, Kim A, Kim J. 2016. Caffeine inhibits adipogenesis through modulation of mitotic clonal expansion and the AKT/GSK3 pathway in 3T3-L1 adipocytes. *BMB Rep **49**: 111–115*.

Table 1. Body and adipose tissue weight of mice with or without CE supplementation

	Control	1% CE
Body weight (g)	28.0 ± 0.3	24.5 ± 0.2**
Tissue weight (g/100g BW)		
Liver	5.89 ± 0.21	5.56 ± 0.33
Total white adipose tissue	3.18 ± 0.17	2.22 ± 0.11**
Mesenteric	0.38 ± 0.08	0.23 ± 0.02
Epididymal	1.01 ± 0.06	0.74 ± 0.03**
Perirenal	0.26 ± 0.01	0.15 ± 0.01**
Subcutaneous	1.38 ± 0.12	0.98 ± 0.12*
Brown adipose tissue	0.45 ± 0.01	0.57 ± 0.03**

Male ICR mice were administered a diet containing 0% (Control) or 1% CE in their tap water for 7 d. Data are presented as the mean ± SE (n = 5), *: $p < 0.05$, **: $p < 0.01$

Table 2. Plasma glucose, lipid, and adiponectin levels of mice with or without CE supplementation

	Control	1% CE
Blood glucose (mg/dL)	121 ± 4	111 ± 5
Plasma cholesterol (mg/dL)	101 ± 10	88 ± 7
Plasma triacylglycerol (mg/dL)	124 ± 7	68 ± 5**
Plasma adiponectin (ng/mL)	73 ± 6	106 ± 8**

Male ICR mice were administered a diet containing 0% (Control) or 1% CE in their tap water for 7 d. Data are presented as the mean ± SE (n = 5), **: $p < 0.01$

Figure Legends

Figure 1. Effect of CE on lipid accumulation in 3T3-L1 adipocytes. (A) Sudan II staining of lipid droplets in 3T3-L1 cells. The cells were incubated with CE at various concentrations in the presence or absence of DMI for 6 d, and lipid droplets were stained with Sudan II (upper panels). The stained lipid droplets in the cells were quantified (bottom panel). Data are presented as the mean ± SE (n = 3), and the lipid content is shown based on a sample from cells cultured in the absence of DMI and CE. (B) Cell viability of 3T3-L1 cells following treatment with CE. After 3T3-L1 cells were incubated with the indicated concentrations of CE in the presence of DMI for 72 h, the cell viability was determined by crystal violet staining assays. Data are presented as the mean ± SE (n = 3). Different letters indicate statistically significant differences (p < 0.05).

Figure 2. Effect of CE on the protein and mRNA expression of PPARγ and C/EBPα in 3T3-L1 adipocytes.
3T3-L1 cells were incubated with the indicated concentrations of CE in the presence of DMI for 6 d. (A–B) Protein (A) or mRNA (B) expression of PPARγ (*Pparg*) and C/EBPα (*Cebpa*) was measured by Western blotting and qPCR, respectively. For protein expression, β-actin was used as a loading control. The intensity of each band was

690 quantified by ImageJ 1.44, and the ratio of each target band level
691 was normalized to the β-actin level. For mRNA expression, the
692 value of *Gapdh* was used as an internal control. Data are presented
693 as the mean ± SE (n = 3), and relative values are shown based on a
694 sample from cells cultured in the absence of DMI and CE. Different
695 letters indicate statistically significant differences ($p < 0.05$).
696
697 Figure 3. Effect of CE on the protein expression levels of C/EBPβ
698 and C/EBPδ in 3T3-L1 adipocytes.
699 3T3-L1 cells were incubated with the indicated concentrations of CE
700 in the presence of DMI for 24 h. Protein expressions of C/EBPβ and
701 C/EBPδ were measured by Western blotting. β-actin was used as a
702 loading control. The intensity of each band was quantified by
703 ImageJ 1.44, and the ratio of each target band level was normalized
704 to the β-actin level. Data are presented as the mean ± SE (n = 3),
705 and the relative values are shown based on a sample from cells
706 cultured in the absence of DMI and CE. Different letters indicate
707 statistically significant differences ($p < 0.05$).
708
709 Figure 4. Effect of CE on the protein expression of SREBP-1 and
710 FAS and the cellular localization of SREBP-1 in 3T3-L1 adipocytes.
711 3T3-L1 cells were incubated with the indicated concentrations of CE
712 in the presence of DMI for 6 d. (A) Protein expressions of SREBP-1
713 and FAS were measured by Western blotting. β-actin was used as a

714 loading control. The intensity of each band was quantified by
715 ImageJ 1.44, and the ratio of each target band level was normalized
716 to the β-actin level. Data are presented as the mean ± SE (n = 3),
717 and relative values are shown based on a sample from cells cultured
718 in the absence of DMI and CE. Different letters indicate statistically
719 significant differences ($p < 0.05$). (B) Localization of SREBP-1 was
720 determined by fluorescence microscopy. SREBP-1 was stained with
721 Alexa 488, and the nuclei were counterstained with DAPI.
722
723 Figure 5. Effect of CE on the protein expression of PPARγ and
724 C/EBPs in mesenteric white adipose tissue of mice.
725 Male ICR mice were provided a diet containing 0% or 1% CE in tap
726 water for 7 d. The protein expressions of PPARγ, C/EBPα, C/EBPβ
727 and C/EBPδ were measured by Western blotting. Each panel shows a
728 typical result from five animals. β-actin was used as a loading
729 control. The intensity of each band was quantified by ImageJ 1.44,
730 and the ratio of each target band level was normalized to the β-actin
731 level. Data are presented as the mean ± SE (n = 5), and relative
732 values are shown based on the control group. Different letters
733 indicate statistically significant differences ($p < 0.05$).
734
735 Figure 6. Effect of CE on the protein expression of SREBP-1 and
736 Fas in the mesenteric white adipose tissue of mice.
737 Male ICR mice were provided with a diet containing 0% or 1% CE

738 in tap water for 7 d. Protein expressions of SREBP-1 and Fas were
739 measured by Western blotting. Each panel shows a typical result
740 from five animals. β-actin was used as a loading control. The
741 intensity of each band was quantified by ImageJ 1.44, and the ratio
742 of each target band level was normalized to the β-actin level. Data
743 are presented as the mean ± SE (n = 5), and relative values are
744 shown based on the control group. Different letters indicate
745 statistically significant differences ($p < 0.05$).
746
747 Figure 7. Effect of CE on the levels of AMPK phosphorylation and
748 ACC expression in the mesenteric white adipose tissue of mice.
749 Male ICR mice were provided with a diet containing 0% or 1% CE
750 in tap water for 7 d. AMPK phosphorylation and ACC expression
751 were measured by Western blotting. Each panel shows a typical
752 result from five animals. The expression level of each protein was
753 also measured. The intensity of each band was quantified by ImageJ
754 1.44, and the ratio of the phosphorylation level was normalized to
755 the expression level. Data are presented as the mean ± SE (n = 5),
756 and relative values are shown based on the control group. Different
757 letters indicate statistically significant differences ($p < 0.05$).
758

Figure 1

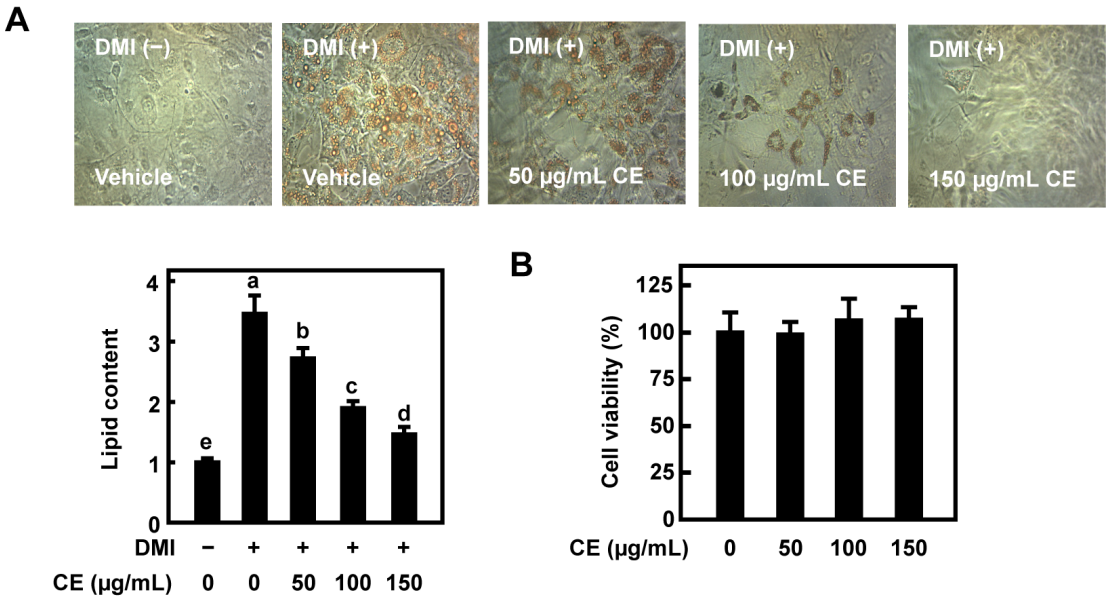
A
DMI (−)
Vehicle
DMI (+)
Vehicle
DMI (+)
50 μg/mL CE
DMI (+)
100 μg/mL CE
DMI (+)
150 μg/mL CE
Lipid content
0
1
2
3
4
a
b
c
d
e
DMI − + + + +
CE (μg/mL) 0 0 50 100 150
B
Cell viability (%)
0
25
50
75
100
125
CE (μg/mL) 0 50 100 150

Figure 2

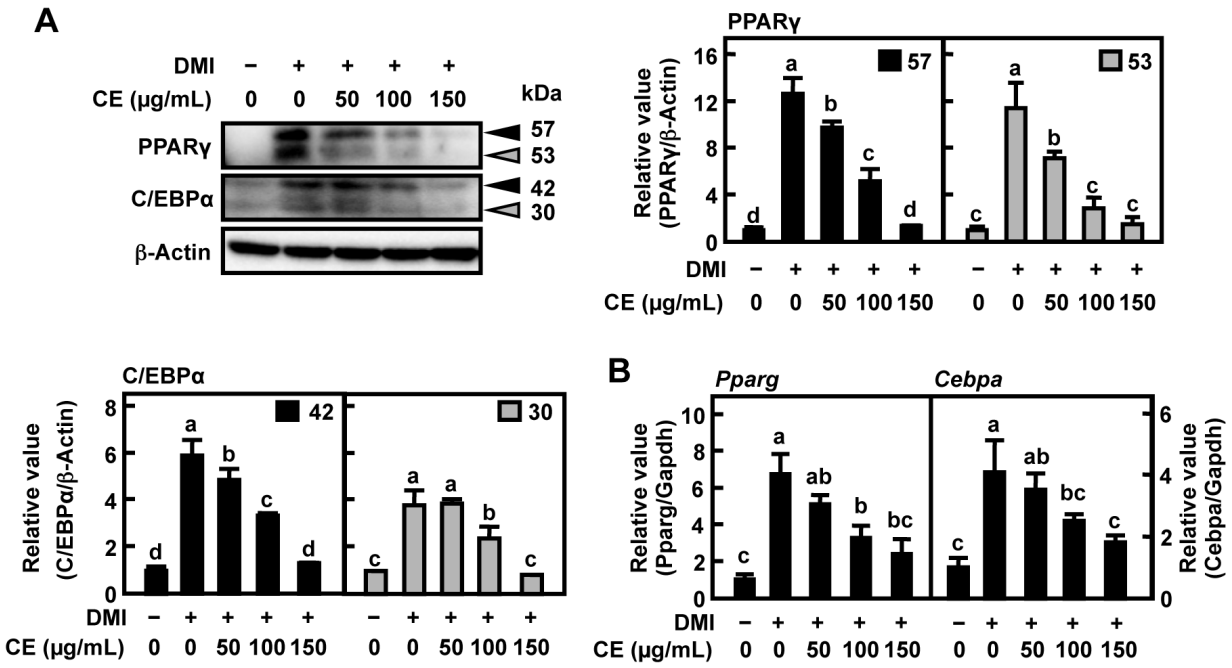
A
DMI
CE (μg/mL)
kDa
PPARγ
C/EBPα
β-Actin
57
53
42
30
PPARγ
Relative value (PPARγ/β-Actin)
C/EBPα
Relative value (C/EBPα/β-Actin)
B
Pparg
Cebpa
Relative value (Pparg/Gapdh)
Relative value (Cebpa/Gapdh)

Figure 3

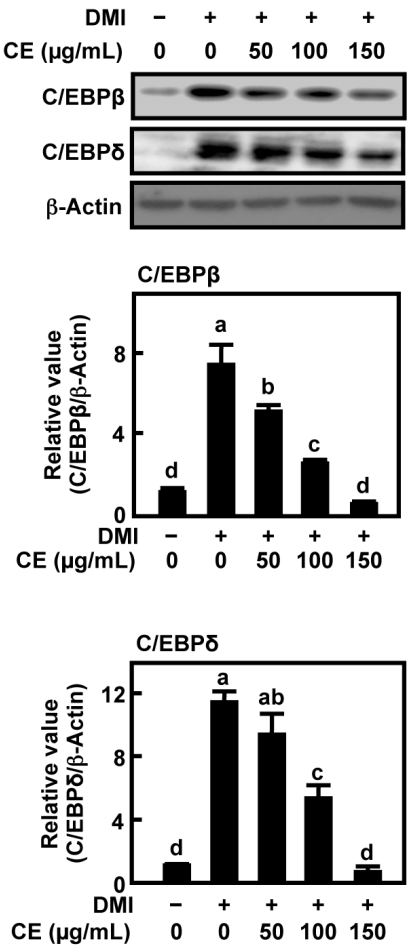
DMI – + + + +
CE (μg/mL) 0 0 50 100 150
C/EBPβ
C/EBPδ
β-Actin
C/EBPβ
Relative value (C/EBPβ/β-Actin)
a
b
c
d
d
8
4
0
DMI – + + + +
CE (μg/mL) 0 0 50 100 150
C/EBPδ
Relative value (C/EBPδ/β-Actin)
a
ab
c
d
d
12
8
4
0
DMI – + + + +
CE (μg/mL) 0 0 50 100 150

Figure 4

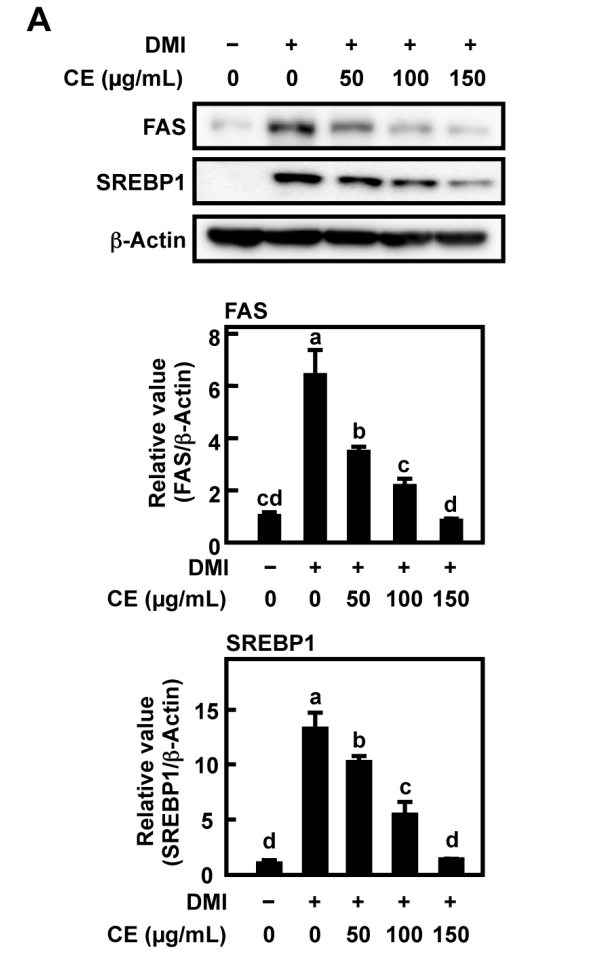
A
DMI – + + + +
CE (μg/mL) 0 0 50 100 150
FAS
SREBP1
β-Actin
FAS
Relative value (FAS/β-Actin)
8
6
4
2
0
a
b
c
cd
d
DMI – + + + +
CE (μg/mL) 0 0 50 100 150
SREBP1
Relative value (SREBP1/β-Actin)
15
10
5
0
a
b
c
d
d
DMI – + + + +
CE (μg/mL) 0 0 50 100 150

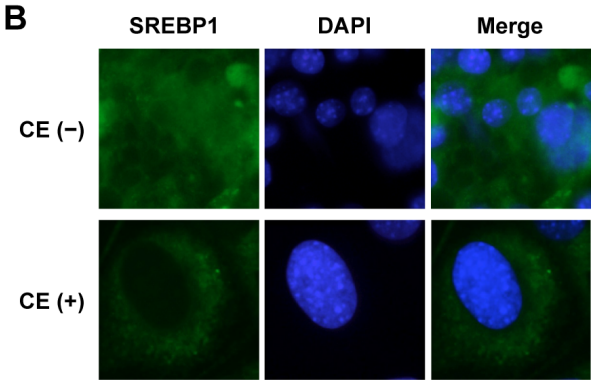
B
SREBP1
DAPI
Merge
CE (−)
CE (+)

Figure 5

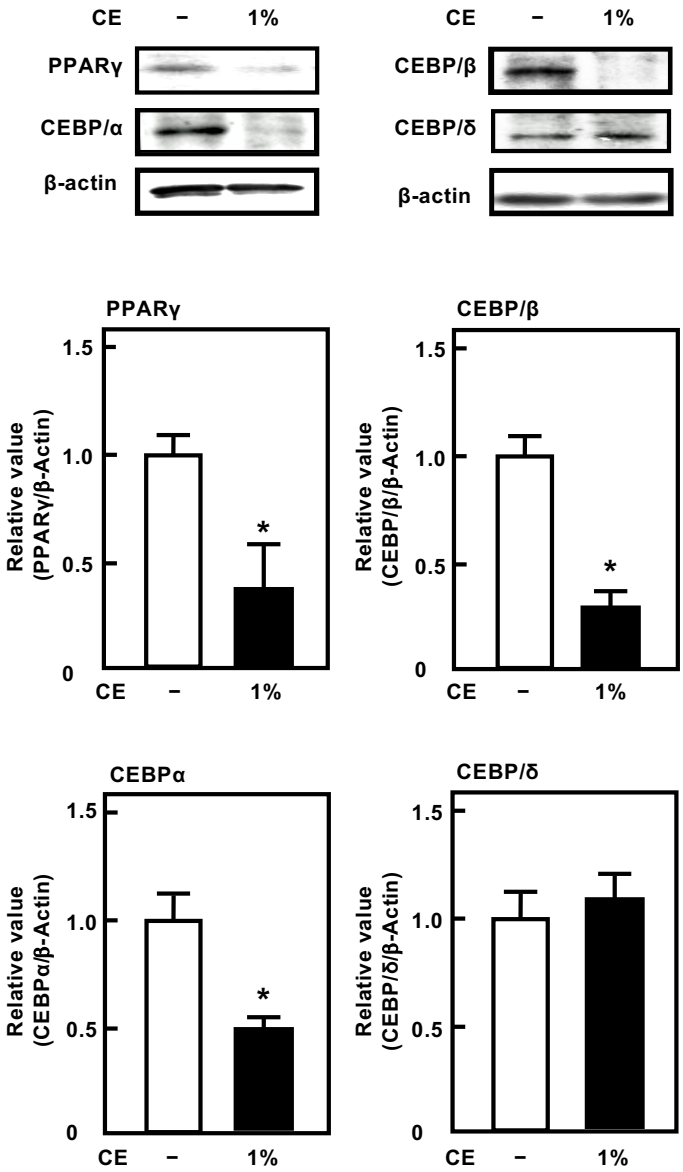
CE
–
1%
PPARγ
CEBP/α
β-actin
CE
–
1%
CEBP/β
CEBP/δ
β-actin
PPARγ
Relative value
(PPARγ/β-Actin)
1.5
1.0
0.5
0
*
CE
–
1%
CEBP/β
Relative value
(CEBP/β/β-Actin)
1.5
1.0
0.5
0
*
CE
–
1%
CEBPα
Relative value
(CEBPα/β-Actin)
1.5
1.0
0.5
0
*
CE
–
1%
CEBP/δ
Relative value
(CEBP/δ/β-Actin)
1.5
1.0
0.5
0
CE
–
1%

Figure 6

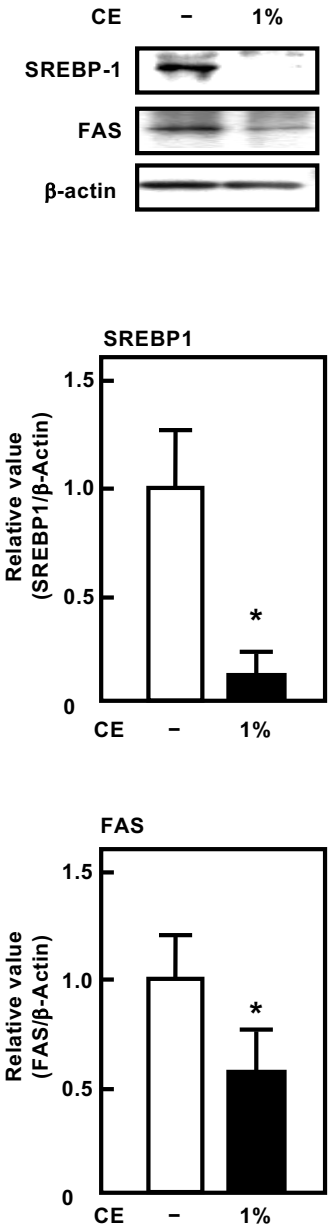
CE
–
1%
SREBP-1
FAS
β-actin
SREBP1
Relative value
(SREBP1/β-Actin)
1.5
1.0
0.5
0
*
CE
–
1%
FAS
Relative value
(FAS/β-Actin)
1.5
1.0
0.5
0
*
CE
–
1%

Figure 7

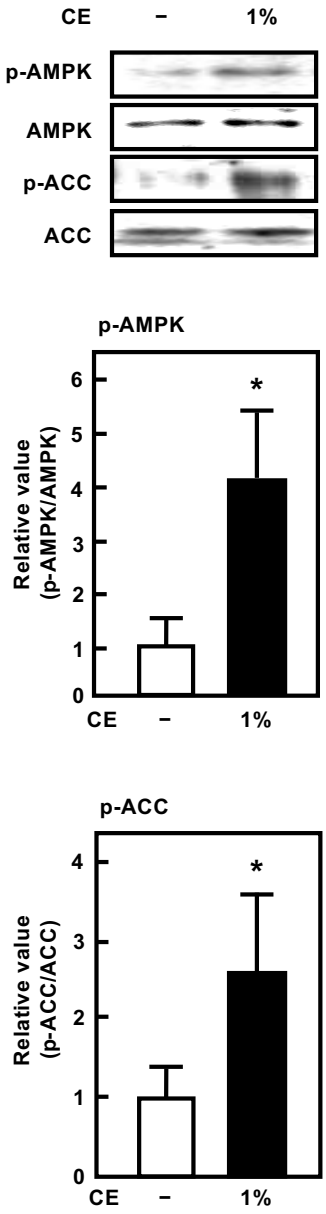
CE
–
1%
p-AMPK
AMPK
p-ACC
ACC
p-AMPK
Relative value
(p-AMPK/AMPK)
0
1
2
3
4
5
6
*
CE
–
1%
p-ACC
Relative value
(p-ACC/ACC)
0
1
2
3
4
*
CE
–
1%